Tellus (1994), 46A, 529–540
Printed in Belgium – all rights reserved

TELLUS
ISSN 0280–6495

Limits to predictability in a coupled ocean-atmosphere model due to atmospheric noise

By RICHARD KLEEMAN* and SCOTT B. POWER, *Bureau of Meteorology Research Centre, G.P.O. Box 1289K, Melbourne 3001, Australia*

(Manuscript received 6 August 1993; in final form 29 December 1993)

ABSTRACT

A coupled-ocean atmosphere model with demonstrated skill in ENSO prediction is used to examine limits to predictability due to stochastic momentum forcing from the atmosphere. Previous estimates of predictability limits in coupled models may be overly optimistic because of the absence of realistic atmospheric noise in the intermediate atmospheric model used. It is found that unavoidable error grows rapidly with a time scale of 4 or so months. It then saturates at a level around 0.5°C for the Niño 3 region.

1. Introduction

In the science of weather forecasting, it is now generally accepted (Lorenz, 1982) that there are fundamental limits to predictability which essentially manifest themselves as an extreme sensitivity of predictions to initial conditions. Such sensitivity is not only due to non-linearities in the dynamical system (chaos) which can cause unstable normal modes in the linearized equations but may also be due to the non self-adjointness of the linearized dynamical system (see, for example, Farrell, 1990).

In recent years, successful predictive coupled ocean-atmosphere models of El Niño, Southern Oscillation have appeared (see Zebiak and Cane, 1987 (ZC henceforth); Kleeman, 1993; Latif et al., 1993) and so it is natural to enquire whether similar limits to predictability exist for the ENSO phenomenon. This issue has been addressed in the context of the ZC model by Goswami and Shukla (1991) and also Blumenthal (1991). In both cases, the growth of small perturbations in initial conditions are examined and it is found that error doubling occurs on time scales of a year or so. Both authors assume that on these time scales growth occurs due essentially to linear processes: the first authors postulate that the unstable normal modes of the system are responsible while the second ascribes growth to the non self-adjointness of the system.

The predictability problem has also been examined using the observations of the Southern Oscillation with sophisticated statistical analysis techniques by Fraedrich (1988) who concluded that a stochastic model rather than a strange attractor accounted for the data. He deduced an error doubling timescale of up to one year however this number was somewhat uncertain due to the lack of a sufficiently long dataset.

An obvious limitation of the above two dynamical studies is the simplifications inherent in the ZC model. One such simplification occurs in the atmosphere: It is a steady-state model (there are no time derivatives in the model equations) and is not intended to model the high frequency transients that are an essential feature of the tropical atmosphere. In some sense one can regard this atmospheric model as a slave to its lower boundary condition (the sea-surface temperature anomaly) and therefore incapable of generating *realistic* internal variability. Although there has been some discussion in the literature (Battisti, 1988, for example) concerning noise generated in the model by its moisture convergence feedback mechanism, it seems unlikely, given the mathe-

* Corresponding author.

matical formulation, that it is either realistic or large enough.

In the present study, we shall use the simple coupled model due to Kleeman (1993) whose atmosphere is also a steady state model (see Kleeman, 1991). In order to examine the influence of the high frequency transients in the tropical atmosphere, the Florida State University (FSU) pseudo-windstress dataset will be high pass filtered at an appropriate cutoff frequency (to be discussed further below) and added to the atmosphere. If one assumes that such an atmospheric signal is intrinsically unpredictable beyond a month or so* then a fundamental limitation emerges in ENSO predictability as different realizations of the "noise" will induce different trajectories in the phase space of the coupled model. It is the extent of this divergence of trajectories that will be examined here.

This situation is analogous to one which has been examined in the atmospheric context by, for example, Egger and Schilling (1984). There it is assumed that the planetary scale modes are forced by the synoptic scale modes which are represented by red noise. Such a study is undertaken to examine the degree to which the low frequency/large scale part of the circulation (as opposed to the total circulation) is predictable given the presence of "noise" which is only predictable on quite short time scales. In some respects, the present works seperation of "modes" into dynamics and noise is more natural since it is based on the greatly differing natural timescales of the ocean and atmosphere.

The paper is organized as follows: Section 2 contains a description and performance assessment of the models utilized together with a description and analysis of the noise dataset to be used. Section 3 contains the experimental design for examining the predictability implications of the noise together with the results, while Section 4 contains a discussion and suggestions for future work.

2. Model description and behaviour and the noise dataset

The atmospheric model used in this study has been described in detail in Kleeman (1991). We provide a brief review here and refer the interested reader to the relevant article.

The 750 mb anomalous winds are given by a steady state Gill (1980) type model of the equatorial β-plane:

$$\begin{aligned} \varepsilon u - fv &= -\Phi_x, \\ \varepsilon v + fu &= -\Phi_y, \\ \varepsilon\Phi + c^2 \nabla \cdot \boldsymbol{u} &= -\tfrac{1}{2} R[\varepsilon T + Q_m], \end{aligned} \tag{1}$$

where Φ is the anomalous geopotential, T is the boundary layer temperature anomaly (assumed to equal the SST anomaly), R is the gas constant, ε is a Rayleigh friction and Newtonian cooling relaxation parameter with value approximately $(2\text{ days})^{-1}$, c is the atmospheric shallow water speed with value 60 ms^{-1} and Q_m is the mid tropospheric latent heating. The model is therefore forced by a direct thermal heating and a latent heating from deep convective anomalies. The latter heating is obtained using firstly a 28°C SST cutoff:

$$\begin{aligned} Q_m &= \max\{Q_c - \bar{Q}_p\} && \text{SST} > 28°\text{C} \\ &= -\bar{Q}_p && \text{otherwise,} \end{aligned} \tag{2}$$

where $\bar{Q}_p$ is the climatological penetrative precipitation latent heating (obtained from the observed OLR data). Q_c is the anomalous heating caused by changes in moisture and circulation which derive from SST anomalies. Q_c is obtained from the vertically integrated moisture equation under 3 assumptions:

(1) all relevant variables have a fixed vertical structure;

(2) $T = \text{SST} - 1.5°\text{C}$; 80% near surface relative humidity;

(3) the moisture tendency is assumed to be negligible, in other words, a steady state moisture equation is assumed.

These assumptions allow one to solve the moisture equation for anomalous precipitation which is used to calculate Q_c. In simple terms, the model takes an SST anomaly which causes a direct thermal forcing of eq. (1) and then by feedback a much larger latent heating forcing, and produces a wind field anomaly. The model has a strong tendency to locate heating anomalies (and hence wind anomalies) in regions of high total SST. This is due to eq. (2) and also because the moisture

* This would appear to be an optimistic upper limit given current tropical NWP capability.

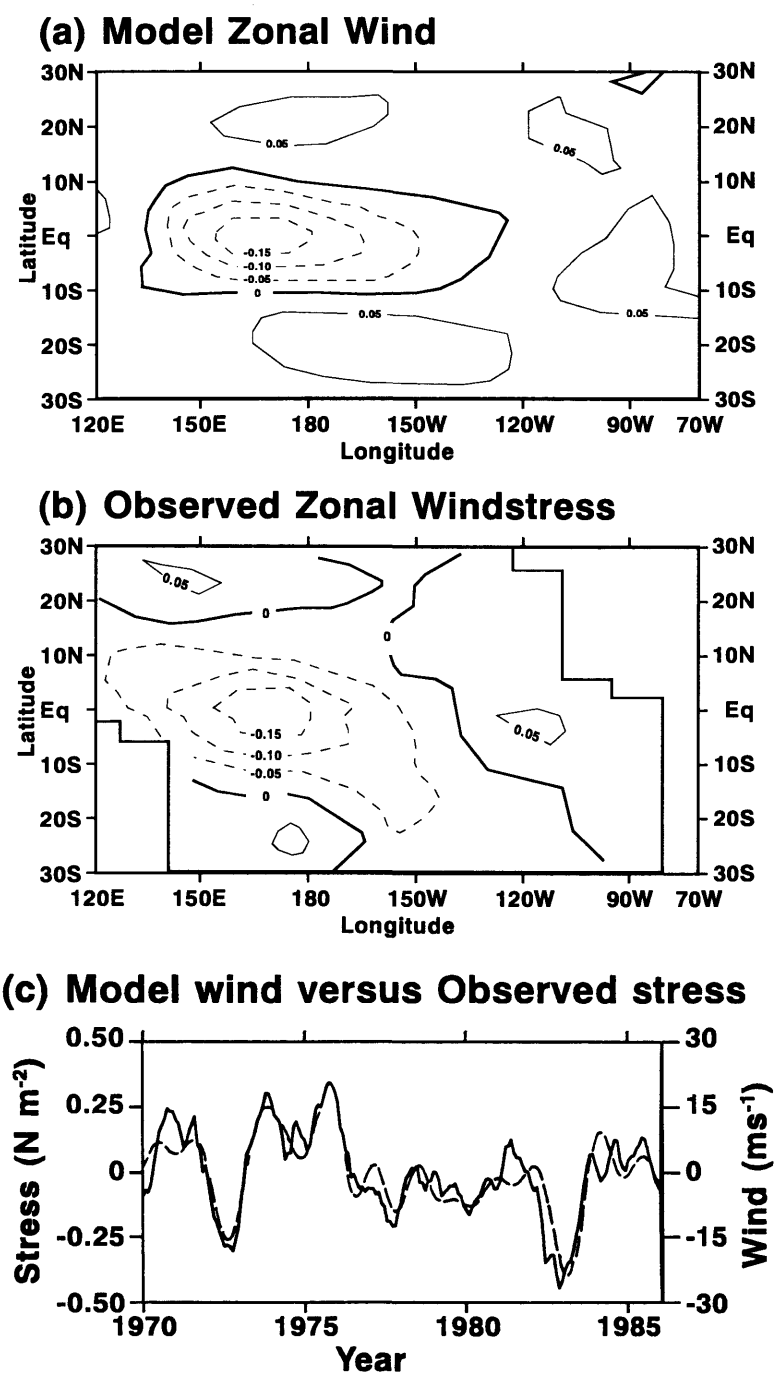

Fig. 1. (a) The spatial pattern for the atmospheric models' first EOF of zonal wind. (b) As for (a) but for the observed zonal windstress. (c) The component timeseries for the spatial patterns in (a) and (b). Observed stress is the dashed line while the solid line is modeled wind; multiplying the values here by those in (a) and (b) results in stress (Nm^{-2}) and wind (ms^{-1}).

feedback parameter (see Zebiak, 1986) is a function of the total SST implying that the process of moisture feedback which induces most of the heating in the model is more efficient in high SST regions.

Model performance is good where interannual variations are concerned as can be seen in Fig. 1. Displayed is a comparison of the first EOF of zonal wind from the model (derived by forcing the model with Climate Analysis Centre (CAC) analyses of SST anomalies from 1970–86) with the observed zonal windstress (from the FSU dataset using $c_d = 1.5 \times 10^{-3}$) with periods less than twelve months filtered out.

As the frequency of variations increases beyond the interannual, agreement between model and observations declines. This can be demonstrated by a cross-spectral analysis. Displayed in Figs. 2a and 2b is such an analysis for the region 5°N–5°S; 160°E–160°W for the quantities of Fig. 1. The phase crudely speaking represents the phase difference in degrees for oscillations of the specified frequency while the coherence the correlation of signals with the specified frequency. This analysis has been repeated for other regions of the Pacific with qualitatively similar results (the coherency of longer periods tends to be somewhat less in other regions presumably because the signal is smaller and there is lesser agreement between model and observations as a result). As can be seen, the coherency and phase show good agreement between model and observations at longer periods and poor agreement for periods less than 15 months.

Not only is there little agreement between model and observations at such high frequencies but there is also a big difference in the spectrum as can be seen in Fig. 2c. Here the model zonal wind has been converted to an equivalent zonal stress using a linearized stress law with a mean windspeed of 6.5 ms^{-1} (see eq. (5) below). The observations show an essentially flat (or white) spectrum below about a year while the model spectral intensity is much less and slightly redder*. At longer periods ($> \sim 1.5$ years) the spectra (not shown) are in quite close agreement. An obvious interpretation of these results is that the model contains little

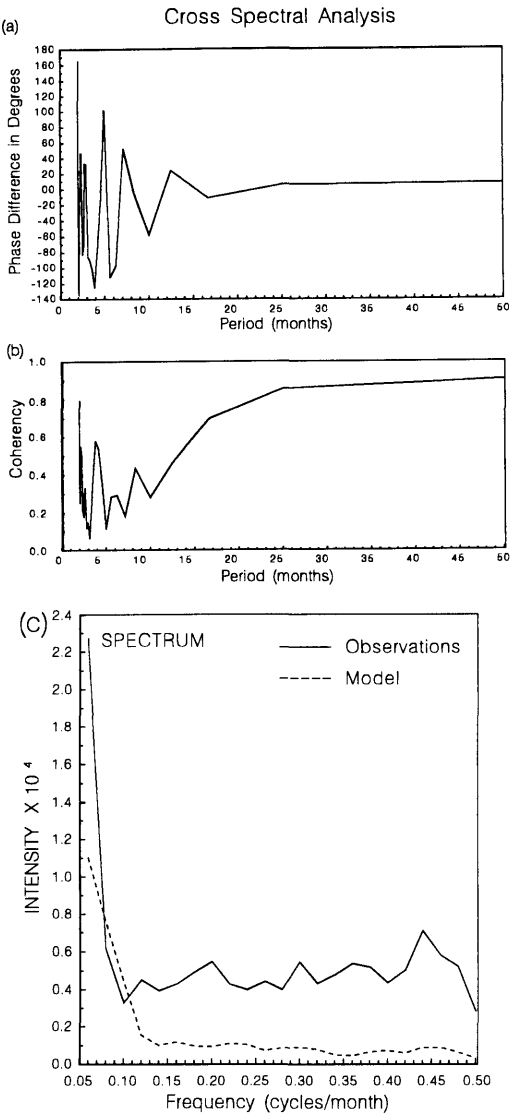

Fig. 2. (a) The cross spectral coherency and (b) phase difference (in degrees) between the observed zonal windstress and modeled zonal wind in the region 5°N–5°S; 160°E–160°W. (c) The spectra of the modelled and observed zonal windstress for the same region. Units for the spectral intensity are $(Nm^{-2})^2$.

of the high frequency noise found in the real atmosphere. Such an interpretation needs to be tempered somewhat by the reality that some of the high frequency noise evident in the FSU dataset is probably due to analysis inaccuracies caused by data sparsity. Despite this reservation it seems

* The weak red structure is possibly inherited from the ocean SST, see Hasselmann (1976).

plausible that a large amount of the signal is due to the internally generated transients which are evident in the tropical atmosphere (see WCRP, 1990).

In order to ascertain the influence of this noise on coupled model predictability, we adopt the simplest possible strategy: The FSU data is high pass filtered with a cutoff of 12 months period. This cutoff corresponds to the approximate "break point" seen in the observational spectrum of Fig. 2c: Above this frequency the spectrum has a fairly uniform white character. Note that such a cutoff also corresponds with the point at which coherency and phase between model and observations shows a rapid change.

The noise is a significant part of the observations as can be seen in Fig. 3 where its' zonal windstress standard deviation is displayed. Values of 0.025 Nm^{-2} are typical and these compare with peak interannual zonal windstress anomalies in the full observational dataset of 0.05 Nm^{-2} to 0.1 Nm^{-2}. Another interesting aspect is the significant spatial character of the variance, in general it is higher in regions of greater mean stress. This result might be expected given the quadratic nature of the stress law: a given wind anomaly will result in a larger stress anomaly in regions of larger climatological wind.

The degree to which the noise dataset is unpredictable can be roughly judged by computing the point wise auto correlation function for lags of 1, 3 and 6 months. Small negative correlations at short lags give way to near zero values at 6 months. Such a result is consistent with white noise that is truncated at 1 and 12 months. The autocorrelation function for such noise is easily computed by taking the Fourier transform of the spectrum (see Priestley, 1981) with the result:

$$c(\tau) \propto -\frac{1}{\tau}\sin\left[\frac{2\pi\tau}{12}\right], \tag{3}$$

where τ is the time lag in months. The behaviour of the autocorrelation for varying lags is thus consistent with eq. (3). On the basis of this we conclude therefore that the prediction of the noise dataset signal beyond one month is essentially impossible. This is consistent with the philosophy outlined in the previous section.

In Kleeman (1993), the atmospheric model above is coupled to a range of ocean models. The anomaly ocean model to be used in the current experiments is the one from this reference which gives the optimal hindcast skill in ENSO prediction. A detailed description of the ocean model together with an analysis of the hindcast skill of the coupled model can be found in the above reference. We confine ourselves here to a brief description: The ocean model relies solely on thermocline perturbations and the meridional structure of SST anomalies is Gaussian about the equator with an e-folding width of 10°. Thus SST is entirely determined by what happens on the equator. The SST anomaly equation there may be written as

$$T_t = \alpha(x)\,\theta(h) - \gamma T, \tag{4}$$

where T is the SST anomaly, h is the thermocline perturbation in meters, γ is a Newtonian damping coefficient with value (42 days)$^{-1}$ and α and θ are

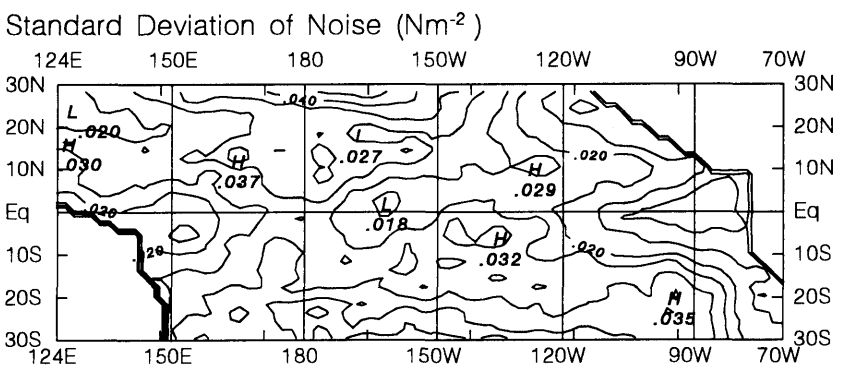

Fig. 3. The standard deviation of the zonal windstress from the noise dataset used in predictability experiments. The contour interval is 0.005 Nm^{-2}.

functions whose forms are displayed in Fig. 4. α describes the zonal variations of the thermocline influence on SST while θ gives an amplitude limiting non-linearity to the model. (If $|h| > h_m$ the influence of h on T is as it would be if equality held). Cane (1984) has shown that observed sea-level variations, which are closely related to thermocline perturbations, can be modelled using the first two baroclinic modes which satisfy the shallow water equations. The dynamics of the ocean model here approximate this fact by using shallow water equations with a shallow water speed of 2.3 ms^{-1} which is intermediate between the wavespeeds of the first two baroclinic modes. In the coupled model context it is found that such a value is optimal with regard to hindcast skill. The long-wave approximation is made to the shallow water equations for computational ease and because it is assumed that the modes which are filtered by such an approximation are unimportant to coupled behaviour. Windstress anomalies force the momentum equations of the shallow water set with an effective body force depth of 150 m.

The model is coupled to the atmosphere via a linearized stress law:

$$\tau = \rho_a c_d |\bar{W}| \, u, \tag{5}$$

with varying values of the "coupling coefficient" $|\bar{W}|$ (the climatological windspeed). Thus low level winds from the atmospheric model are converted to a stress by eq. (5) and then force the shallow water equations. The thermocline perturbation from these equations is used in eq. (4) to predict an SST anomaly which is then passed back to the atmosphere.

The hindcast skill of the coupled model (with $|\bar{W}| = 6.5\ ms^{-1}$) has been tested for the period 1972–86 and the anomaly correlation of the model (together with persistence) in the Niño 3 region (5°S to 5°N and 150°W to 90°W) is displayed in Fig. 5. A rather remarkable insensitivity of this good hindcast skill to the details of the parameterization used has been found and is detailed in Kleeman (1993). In addition to the extensive sensitivity experiments conducted in this reference, the coupling strength has also been varied (increased to 9.0 ms^{-1}) again with little sensitivity.

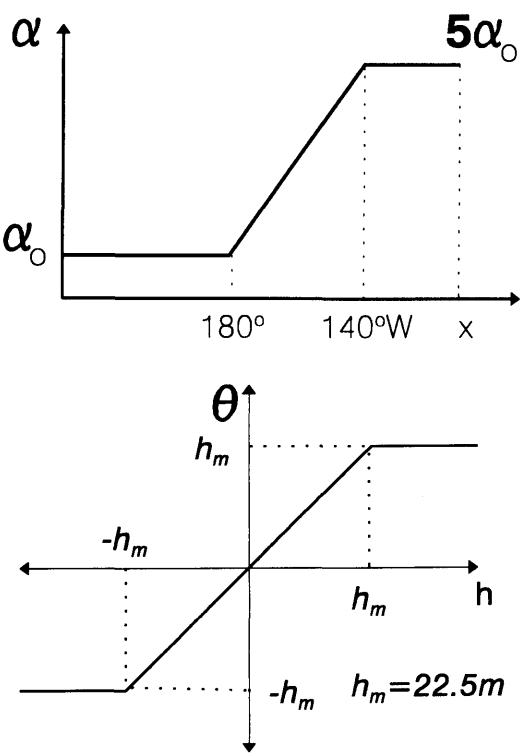

Fig. 4. The form functions used in the model ocean. (a) The function $\alpha(x)$ which gives the zonal dependence of the influence of thermocline perturbations on SST. (b) $\theta(h)$ which gives the non-linearity used in the model.

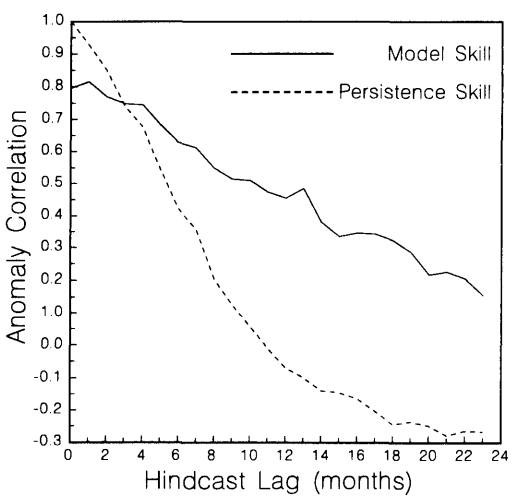

Fig. 5. The anomaly correlation skill of the coupled model for the region of Niño 3 and using a coupling strength of $|\bar{W}| = 6.5\ ms^{-1}$.

3. Predictability experiments

The effect of the noise dataset on predictability was determined as follows (refer simultaneously to Fig. 6): The standard set of hindcast experiments consist of spinning up the ocean model with the observed windstress (the minimum spin up time used was three years) to a series of start dates separated by three months between 1/72 and 7/86 (a total of 59 hindcasts). During each of the 59 2-year coupled hindcasts, 20 different 2-year realizations of the noise dataset were added to the atmospheric model output. In total then, a sample of 1180 two year hindcasts were used in constructing the statistics to be described below. Different realizations of the noise dataset were constructed by randomly choosing a continuous 2-year period from the 30-year dataset (1961–90). The random choice was determined by using a random number generator to select start months for the 2-year realisations.

2 sets of experiments were performed with the coupling strength parameters $|\bar{W}| = 6.5\ \mathrm{ms}^{-1}$ and $9.0\ \mathrm{ms}^{-1}$. The reason for this was the strong dependence of RMS error growth in the model on whether self-sustaining oscillations occur (further detail can be found in Kleeman (1993)). Hovmoeller diagrams of coupled behaviour (commencing July 82), for the 2 different coupling strengths, are displayed in Fig. 7. Notice that while self-sustaining oscillations are present in the high coupling strength case and absent in the low case, the basic structure of the damped oscillation is the same as the self-sustaining one.

Calculation of statistics shall be based on the following philosophy: We shall assume that the model is an adequate realization of the real world coupled system. We shall further assume that one particular coupled model phase space trajectory (induced by a particular realization of the noise) represents the "true" course of the real world coupled system and other trajectories, caused by different noise realizations, represent equally likely trajectories for the coupled system given the specified initial conditions. The mean square unavoidable error E^2 caused by the presence of the

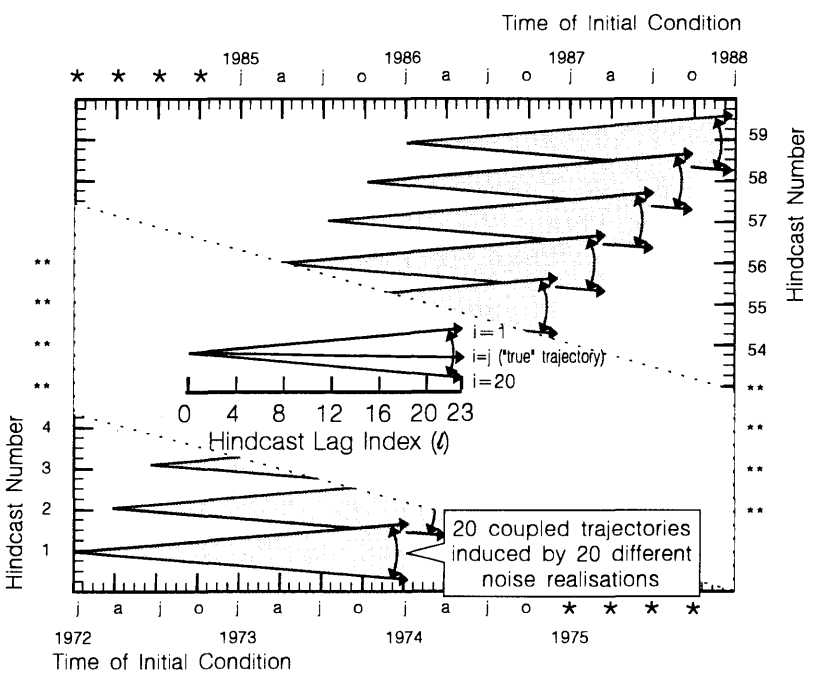

Fig. 6. A schematic of the hindcast experiments used to determine limits to predictability. The index variables *i*, *j* and *k* displayed refer to eq. (6).

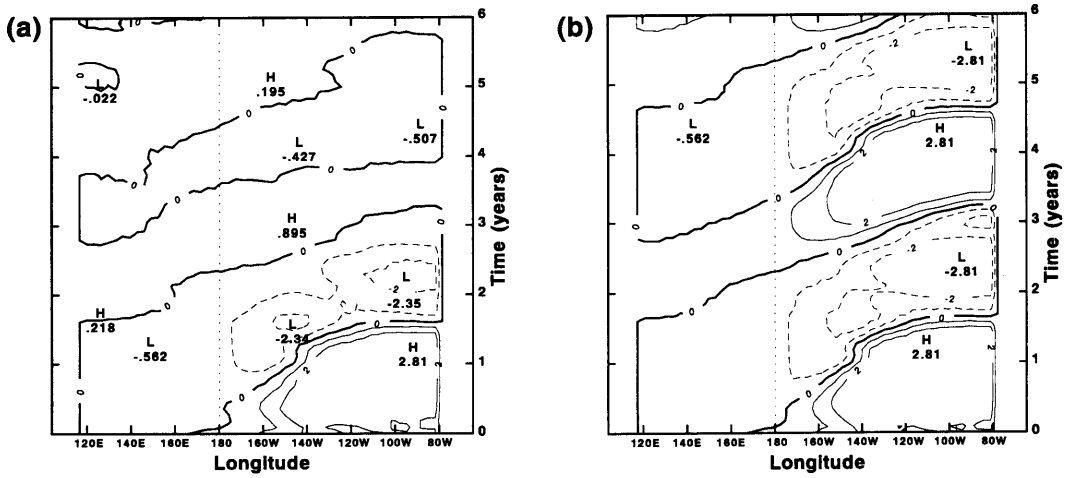

Fig. 7. A longitude-time plot of coupled model SST anomaly behaviour with differing coupling strengths: (a) $|\bar{W}| = 6.5\ \mathrm{ms}^{-1}$ and (b) $|\bar{W}| = 9.0\ \mathrm{ms}^{-1}$. Both model runs were initialised from July 1982.

unpredictable atmospheric noise is therefore estimatable from (refer to Fig. 6):

$$E^2(k, l, j) = \tfrac{1}{19} \sum_{i \neq j} (t_i^k(l) - t_j^k(l))^2 \qquad (6)$$

where $t_i^k(l)$ represents the value of Niño 3 at hindcast lag l (i.e., l months into the hindcast). The superscript k represents the particular initial conditions being considered (i.e., the kth hindcast); the subscripts represent the particular trajectory under consideration with the jth trajectory being considered the "true" one. For a particular set of initial conditions, the expected error can be obtained by averaging E^2 over j (no particular value is to be preferred) and taking the square root. A little manipulation then shows that this error estimate is simply related to the standard deviation SD of Niño 3 for the 20 trajectories

$$E(k, l) = \sqrt{\tfrac{1}{20} \sum_j E^2(k, l, j)} = \sqrt{\tfrac{40}{19}}\, \mathrm{SD}(k, l). \qquad (7)$$

We shall in addition average E^2 with respect to the different initial conditions and then take the square root. This gives a "global" (i.e., under all possible initial conditions) estimate of unavoidable error. We shall term this estimate GUE.

As well as unavoidable error, we shall also compute the "maximal" anomaly correlation (abbreviated as MAC) obtainable in the presence of noise. This is calculated by correlating the 59 member "true" ensemble of hindcasts (i.e., those with subscript j) against another equally likely ensemble (with a fixed subscript i). This is then averaged over all possible values of i and j. Naturally this MAC will be a function of hindcast lag.

Displayed in Fig. 8 are the curves for GUE and also MAC as a function of hindcast lag for the two different coupling strengths. As can be seen, the

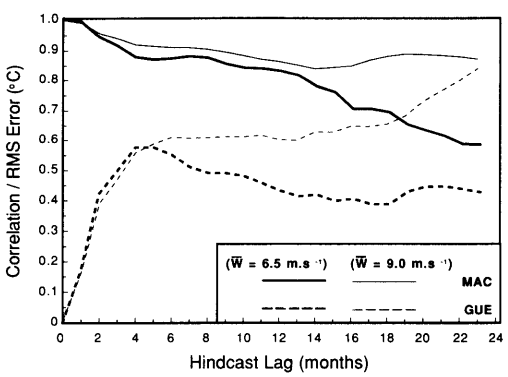

Fig. 8. The global unavoidable error (GUE) (°C) and the maximal anomaly correlation (MAC) (see the text for definition) for the coupling strengths $|\bar{W}| = 6.5\ \mathrm{ms}^{-1}$ and $|\bar{W}| = 9.0\ \mathrm{ms}^{-1}$.

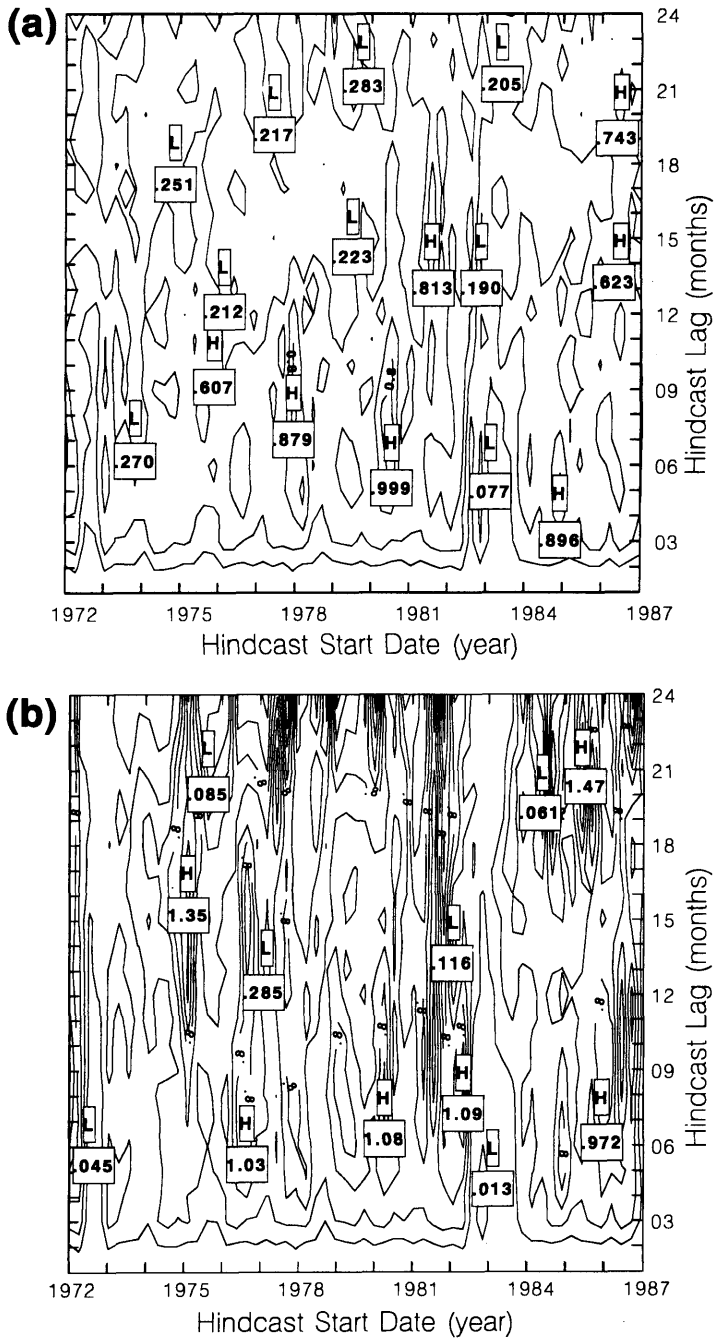

Fig. 9. The dependence of unavoidable error on initial conditions for the coupling strengths (a) $|\bar{W}| = 6.5\ \mathrm{ms}^{-1}$ and (b) $|\bar{W}| = 9.0\ \mathrm{ms}^{-1}$. The contour interval in both cases is 0.2°C. (c) The dependence of $|h| - h_m$ in Niño 3 on the initial conditions of hindcasts and the hindcast lag for the coupled model without noise added and coupling strength $|\bar{W}| = 6.5\ \mathrm{ms}^{-1}$. Values greater than zero indicate that significant non-linearity is operating in the model. Contour interval is 5 m.

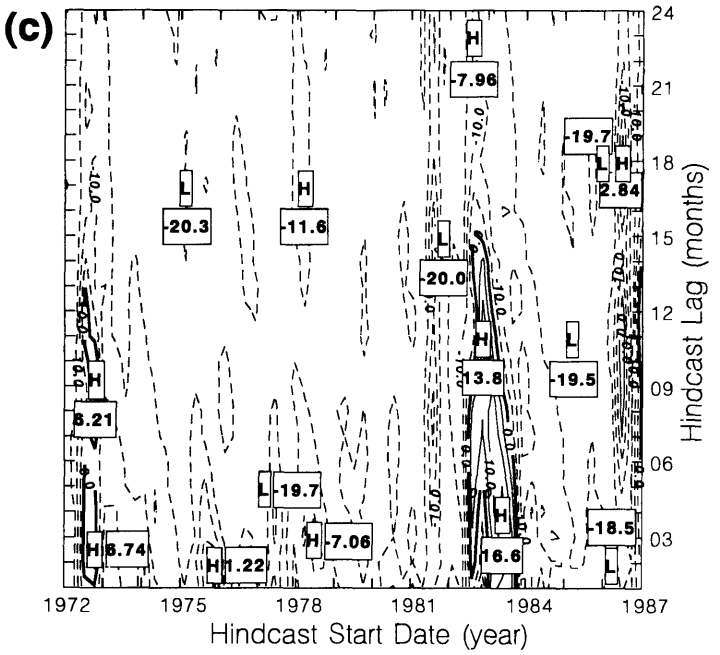

Fig. 9. (cont'd.)

short time-scale behaviour of GUE is relatively insensitive to coupling strength and shows a rapid increase to a level of 0.5°C after 4–5 months. The behaviour at longer lags shows that GUE tends to increase at stronger coupling strengths while a gradual decrease occurs for the weak case. This latter result is what one might expect intuitively from Fig. 7. Interestingly MAC skill shows an "opposite" sensitivity with skill declining more rapidly in the weaker coupling strength case.

The sensitivity of unavoidable error to initial conditions is displayed in Figs. 9a, b. As can be seen, there is an almost universal tendency for rapid initial growth to a level around 0.5°C. The exception occurs during strong warm events (72 and 82/83) where there is much reduced growth of error. The cause of this reduced error growth is to be found in the limiting non-linearity of the coupled model. In Fig. 9c the quantity $|h| - h_m$ is plotted (c.f. Fig. 4) for the Niño 3 region for the case without noise. The close correspondence between the positive regions in Fig. 9c and the low error regions in Figs. 9a, b is quite clear. Why this should be the case is fairly obvious: If $|h| \gg h_m$ then a range of random perturbations will not cause this inequality to be altered implying that there will be no difference to the SST equation for different perturbations and hence no effect on the coupled trajectory. It is interesting that the non-linearity operates more during warm rather than cold events in the coupled model. A possible explanation is the non-linearity of the atmospheric model: It responds more strongly when the *total* SST is greater.

As well as the reduced error growth initial conditions, there are also times when the growth is quite a bit larger than normal. The reasons for this are less clear and are possibly related to times when the basic state of the model is more unstable. There is some tendency for there to be enhanced growth before the onset of warm events.

4. Discussion

We have seen that a robust characteristic of GUE (global unavoidable error) is an initial rapid growth rate followed by an approximate plateau at about 0.5°C for the Niño 3 region. Such behaviour is typical of the type of equation which is obtained by linearizing the coupled model, a stochastic differential equation (see, e.g., Gardiner, 1985). The variance (and hence standard deviation) of such

equations saturates on a timescale determined by the damping timescale of the mode. This suggests that the rapid growth in error here is caused by the stimulation by the noise of coupled modes whose damping timescale is quite short i.e., by relatively "stable" modes. Results from a linearization study involving the analytical solution of a stochastic differential equation will be presented elsewhere along with other issues dicussed below.

It is interesting to compare these results with those of Zebiak (1989) who conducted similar experiments to the ones reported here (with the ZC model) but with an idealised representation of the effect of the 30–50 day oscillation. He found a much smaller GUE than that reported here.

A possible explanation for this difference is that the noise used by Zebiak had its variance confined to a fairly localised region in the western equatorial Pacific while the dataset used here has a spatially much broader variance pattern (c.f. Fig. 4).

As an interesting aside, Goswami and Shukla (1991) noted a rapid increase in RMS error in the CZ coupled model when verified against the *forced model* SST. They speculated that this was due to failings in the model atmosphere (see also Graham et al., 1992). The current study suggests instead that at least part of the rapid initial growth may be due to stochastic processes present in the forced model (remembering that the forcing winds are the noisy "real" winds).

There has been some discussion in the literature on the forcing of aperiodic behaviour by atmospheric noise (Battisti, 1988; Schopf and Suarez, 1988; Goswami and Shukla, 1993). The model used here shows no tendency to develop such behaviour when run out over long periods with the addition of noise. A possibility for the absence of such behaviour is the lack of a seasonal cycle in the ocean model: This is currently under investigation. The implication of such a result, however, is that the present estimate of GUE at longer time lags (order 1 to 2 years) may be over-optimistic since aperiodicity presumably influences predictive skill on time scales comparable with the dominant ENSO one (around 3 years).

A couple of other caveats need to be attached to the conclusions drawn here: The current coupled model, even though it has high hindcast skill and thus captures the dominant mode of ENSO variability, represents a simplification of the real-world coupled system. Presumably the greater range of coupled modes present in the real world could contribute to a somewhat different manifestation of GUE. Secondly, as was noted above, the noise dataset used here has limitations: Undoubtedly some observational uncertainty is manifesting itself as atmospheric noise. We hope to address this issue in the future by using an independent noise dataset. Also the low frequency cutoff of the close to white noise is probably not justifiable. Again this issue will be addressed further at a later date.

The present results suggest that coupled GCMs should show a greater sensitivity to initial conditions than that seen in the CZ model. Results reported by Stockdale (private communication, 1993) seem to confirm this although the presence of noise in other flux components (particularly the heat flux) are probably contributing to the divergence of trajectories in the coupled GCM but evidently do not here.

5. Acknowledgements

The authors wish to thank David Neelin and Mark Cane for useful feedback following presentation of some of the above material at the workshop on the prediction of short range climate variations in Hamburg. One of the authors (R.K.) wishes to thank the Max Planck Institut for the invitation (and financial support) to attend the above workshop. Useful discussions on the subject with Andrew Moore of BMRC are also acknowledged.

REFERENCES

Battisti, D. S. 1988. The dynamics and thermodynamics of a warm event in a coupled atmosphere/ocean model. *J. Atmos. Sci.* **45**, 2889–2919.

Blumenthal, M. B. 1991. Predictability of a Coupled Ocean-Atmosphere Model. *J. Clim.* **4**, 766–784.

Cane, M. A. 1984. Modelling sea level during El Niño. *J. Phys. Oceanogr.* **14**, 1864–1874.

Egger, J. and Schilling, H. D. 1984. Predictability of atmospheric low-frequency motions. In: *Predictability of fluid motions*, ed. G. Holloway and B. J. West. AIP Conf. Proc. no. 106, New York.

Farrell, B. F. 1990. Small error dynamics and the predictability of atmospheric flows. *J. Atmos. Sci.* **47**, 2409–2416.

Fraedrich, K. 1988. El Niño/Southern Oscillation predictability. *Mon. Weath. Rev.* **116**, 1001–1012.

Gardiner, C. W. 1985. *Handbook of stochastic methods.* Springer Verlag, Berlin, 442 pp.

Gill, A. E. 1980. Some simple solutions for heat-induced tropical circulation. *Q. J. R. Meteorol. Soc.* **106**, 447–462.

Goswami, B. N. and Shukla, J. 1991. Predictability of a coupled ocean atmosphere model. *J. Clim.* **4**, 3–22.

Goswami, B. N. and Shukla, J. 1993. Aperiodic variability in the Cane–Zebiak model: a diagnostic study. *J. Clim.* **6**, 628–638.

Graham, N. E., Barnett, T. P. and Latif, M. 1992. Considerations of the predictability of ENSO with a low-order coupled model. *TOGA Notes* **7**, 11–15.

Hasselmann, K. 1976. Stochastic climate models. Part 1: Theory. *Tellus* **28**, 473–485.

Kleeman, R. 1991. A simple model of the atmospheric response to ENSO SST anomalies. *J. Atmos. Sci.* **48**, 3–18.

Kleeman, R. 1993. On the dependence of hindcast skill in a coupled ocean-atmosphere model on ocean thermodynamics. *J. Clim.* **6**, 2012–2033.

Latif, M., Sterl, A., Maier-Reimer, E. and Junge, M. M. 1993. Structure and predictability of the El Niño/Southern Oscillation phenomenon in a coupled ocean-atmosphere general circulation model. *J. Clim.* **6**, 700–708.

Lorenz, E. N. 1982. Atmospheric predictability experiments with a large numerical model. *Tellus* **34**, 505–513.

Priestley, M. B. 1981. *Spectral analysis and time series.* Academic Press, 210–215.

Schopf, P. S. and Suarez, M. J. 1988. Vacillations in a coupled ocean-atmosphere model. *J. Atmos. Sci.* **45**, 549–566.

W.R.C.P. 1990. Scientific Plan for the TOGA coupled ocean-atmosphere experiment. *WCRP Publications Series no. 3*, Addendum, B7–B11.

Zebiak, S. E. 1986. Atmospheric convergence feedback in a simple model for El Niño. *Mon. Weath. Rev.* **114**, 1263–1271.

Zebiak, S. E. 1989. On the 30–60 day oscillation and the prediction of El Niño. *J. Clim.* **2**, 1381–1387.

Zebiak, S. E. and Cane, M. A. 1987. A model El Niño/Southern Oscillation. *Mon. Weath. Rev.* **115**, 2262–2278.